ORIGINAL ARTICLE

Alterations in resting-state functional connectivity after brain posterior lesions reflect the functionality of the visual system in hemianopic patients

Jessica Gallina[1,2] · Marco Zanon[1,2,3] · Ezequiel Mikulan[4] · Mattia Pietrelli[1,2,5] · Silvia Gambino[1,2] · Agustín Ibáñez[6,7,8,9,10] · Caterina Bertini[1,2]

Abstract

Emerging evidence suggests a role of the posterior cortices in regulating alpha oscillatory activity and organizing low-level processing in non-alpha frequency bands. Therefore, posterior brain lesions, which damage the neural circuits of the visual system, might affect functional connectivity patterns of brain rhythms. To test this hypothesis, eyes-closed resting state EEG signal was acquired from patients with hemianopia with left and right posterior lesions, patients without hemianopia with more anterior lesions and healthy controls. Left-lesioned hemianopics showed reduced intrahemispheric connectivity in the range of upper alpha only in the lesioned hemisphere, whereas right-lesioned hemianopics exhibited reduced intra-hemispheric alpha connectivity in both hemispheres. In terms of network topology, these impairments were characterized by reduced local functional segregation, with no associated change in global functional integration. This suggests a crucial role of posterior cortices in promoting functional connectivity in the range of alpha. Right-lesioned hemianopics revealed also additional impairments in the theta range, with increased connectivity in this frequency band, characterized by both increased local segregated activity and decreased global integration. This indicates that lesions to right posterior cortices lead to stronger impairments in alpha connectivity and induce additional alterations in local and global low-level processing, suggesting a specialization of the right hemisphere in generating alpha oscillations and in coordinating complex interplays with lower frequency bands. Importantly, hemianopic patient's visual performance in the blind field was linked to alpha functional connectivity, corroborating the notion that alpha oscillatory patterns represent a biomarker of the integrity and the functioning of the underlying visual system.

Keywords Functional connectivity · Alpha oscillations · Theta oscillations · Resting state · Hemianopia

✉ Caterina Bertini
caterina.bertini@unibo.it

1 Centre for Studies and Research in Cognitive Neuroscience, University of Bologna, Cesena, Italy

2 Department of Psychology, University of Bologna, Bologna, Italy

3 Neuroscience Area, International School for Advanced Studies (SISSA), Trieste, Italy

4 Department of Biomedical and Clinical Sciences "L. Sacco", University of Milan, Milan, Italy

5 Department of Psychiatry, University of WI–Madison, Wisconsin, USA

6 Latin American Brain Health (BrainLat), Universidad Adolfo Ibáñez, Santiago, Chile

7 Cognitive Neuroscience Center (CNC), Universidad de San Andrés, Buenos Aires, Argentina

8 National Scientific and Technical Research Council (CONICET), Buenos Aires, Argentina

9 Global Brain Health Institute, University of California-San Francisco, San Francisco, CA, USA

10 Trinity College Dublin, Dublin, Ireland

Introduction

Cognitive functioning is a distributed and dynamic process, requiring functional interactions among neural populations widely distributed in cortical and subcortical networks. Such interactions between local and remote brain regions have been effectively studied in the domain of EEG research by functional connectivity, measuring the statistical interdependencies between EEG rhythms in a condition of resting state, between different pairs of electrodes (Stam 2010; Aertsen et al. 1989). This electrophysiological marker of functional coupling is able to capture relationships among different brain regions, which are essential for brain functioning (Varela et al. 2001; Tononi and Edelman 1998). In line with this perspective, studies on the healthy brain have shown that spontaneous EEG fluctuations in the resting brain are typically highly organized and coherent (Greicius et al. 2003). More recent findings have also described the complexity of brain connectivity using graph theory (Strogatz 2001), a mathematical approach that quantifies topological properties of neural networks, defining a complex system of nodes (vertices) and edges (links), whose functional activity is characterized by a balance between local specialization and global integration (Ma et al. 2021; Stam, et al. 2007; Tononi, et al. 1994).

A variety of neurological (Parra et al. 2017; Dottori et al. 2017; Babiloni et al. 2008, 2016; Melloni et al. 2015; Rossini et al. 2007) and psychiatric (Barttfeld et al. 2014, 2013; Fingelkurts et al. 2007; Dawson 2004; Haig et al. 2000) conditions have demonstrated to be associated to alterations of the typical pattern of functional connectivity, suggesting that these indices might represent a reflection of neural integrity. In line, investigations in patients with brain lesions have shown a wide range of post-lesional changes in functional connectivity in different frequency bands. Changes in the low-frequency bands (delta/theta) were mainly reported in terms of an increase in the number (Castellanos et al. 2010) and the functionality (Dubovik et al. 2012; Castellanos et al. 2010) of the connections in patients with acquired brain lesions, compared to controls, whereas reports on post-lesional changes in higher frequency bands (e.g., beta) were rather scarce and mostly associated to task-related oscillatory activity (Guggisberg, et al. 2015). In contrast, various patterns of changes have been reported in the alpha range at rest, showing both a post-lesional reduction of brain connectivity, especially in the ipsilesional hemisphere (Dubovik et al. 2012; Westlake et al. 2012; Wu et al. 2011; Castellanos et al. 2010) and in interhemispheric interactions (Wu et al. 2011), but also increased alpha connectivity in the contralesional hemisphere (Westlake et al. 2012) or in the intact regions

of the lesioned hemisphere (Wu et al. 2011; Guggisberg et al. 2008). Moreover, post-stroke reduced functional connectivity in the alpha band has also been related to more severe deficits in functional outcomes (Guggisberg et al. 2015; Dubovick et al. 2012). Similarly, graph theory analyses have also described rearrangements of network topology following stroke, disrupting the balance between local and global processing (Caliandro et al. 2017). More precisely, among others graph theoretical parameters, clustering coefficient (C), reflecting an index of functional segregation, and characteristic path length (L), measuring functional integration, have been shown to be often altered in patients with brain lesions (Vecchio et al. 2019a; 2019b; Caliandro et al. 2017), suggesting decreased functioning efficiency (Achard, et al. 2006).

Despite the increasing evidence of alterations of the electrophysiological functionality of brain networks after brain lesions, the variety of clinical and lesional profiles in the existing literature has concurred to provide only partial and unselective proofs of changes in post-lesional connectivity at rest so far. Indeed, recent findings, investigating oscillatory activity during resting state in hemianopic patients have suggested that posterior lesions, targeting the structures of the visual pathways and resulting in visual field defects (Grasso, et al. 2020a, b), might induce specific alterations in oscillatory patterns. More precisely, posterior brain lesions in hemianopic patients have been shown to selectively reduce the alpha peak and power during rest, while the same was not observed after lesions to anterior regions (Pietrelli et al. 2019), suggesting a role of posterior cortices in generating and distributing alpha oscillatory activity at rest. Moreover, evidence has shown that lesions to posterior cortices (and not lesions to anterior cortices) alter also the typical alpha power reduction observed in the transition from the eyes-closed resting state to the opening of the eyes (i.e., alpha reactivity; Gallina, et al. 2021). Interestingly, when alpha reactivity was more severely impaired after right posterior lesions, a concurrent disruption in reactivity in the theta range at the opening of the eyes was also observed (Gallina et al. 2021). This converging evidence suggests a role of posterior cortices in orchestrating these oscillatory patterns at rest, both coordinating widespread alpha oscillatory activity and organizing focal processing in the theta range and that lesions to these cortices and impairing the visual system might selectively disrupt this oscillatory activity. In line with this view, the relevance of posterior cortices in oscillatory activity, namely in the alpha range, has been widely reported. Occipito-parietal regions, indeed, typically show prominent oscillatory activity in the alpha range (7–13 Hz) during resting state (Rosanova et al. 2009) and have been reported to play a pivotal role in generating alpha oscillations (Thut et al. 2011; Bollimunta et al. 2008). In addition, activity in the alpha range has been reported to be linked to

the excitability of the visual cortices (Romei et al. 2008a, b) and to be associated to aware (Pfurtscheller, et al. 1994) and unaware (Grasso, et al. 2020a, b) visual processing and visuo-spatial attention (Capilla, et al. 2014). In this perspective, oscillations in the alpha range have been suggested to reflect, even at rest, the activity of the underlying neural populations (Sadaghiani and Kleinschmidt 2016; Klimesch et al. 2007) and, thus, the functionality of the visual system. Moreover, alpha oscillations, propagating from posterior visual cortices to higher order cortical sites (Hindriks et al. 2015), might play a special role in coordinating widespread oscillatory activity and orchestrating focal processing in non-alpha frequency bands.

As a consequence, in light of the importance of posterior cortices in generating, distributing and coordinating oscillatory patterns (Hindriks et al. 2015; Thut et al. 2011; Bollimunta et al. 2008; Romei, et al. 2008a, b), it is of great interest to study the effects of lesions to these cortices on oscillations also at the network level. Indeed, as previously mentioned, evidence on hemianopic patients has shown that lesions to posterior cortices alter oscillatory activity at rest and that these alterations might represent a biomarker of the functionality of the visual system (Pietrelli et al. 2019; Gallina et al. 2021). However, it is still unknown whether lesions to posterior cortices might also induce specific post-lesional alterations of functional connectivity patterns in different frequency bands during resting state. Recent human fMRI studies on hemianopic patients showed a decrease in brain functional connectivity, particularly evident in the Visual Network (Pedersini et al. 2020), suggesting that lesions to posterior cortices might affect connectivity, but providing no insight on possible alterations in connectivity in specific frequency bands. Moreover, preliminary EEG investigations showed the presence of some altered patterns of connectivity in the alpha range (Guo et al. 2014; Wang et al. 2012) and suggested that impaired alpha connectivity at rest is predictive of the severity of the visual field deficits (Allaman et al. 2021) after lesions to the visual cortices, but the consequences of posterior lesions on the complex pattern of alpha and non-alpha (e.g. theta) oscillatory processing at rest still needs to be elucidated. Moreover, previous investigations have revealed a different impact of posterior left and right lesions on resting oscillations, with right-damaged hemianopics showing a more severe impairments in alpha peak and in the distributions of alpha power (Pietrelli et al. 2019) and a greater dysfunction in oscillatory reactivity at the opening of the eyes (Gallina et al. 2021). Therefore, the present study aims at investigating whether posterior lesions affect the complex pattern of functional connectivity in different frequency bands and whether lesions to the left or the right hemisphere can differentially alter connectivity patterns.

To explore these hypotheses, EEG activity during eyes-closed resting state was recorded in patients with left or right lesions to the posterior cortices, in control patients with left or right more anterior lesions and in a group of healthy controls. Intrahemispheric and interhemispheric connectivity indices were computed to measure post-lesional functional connectivity changes. In addition, clustering coefficient (C) and characteristic path length (L) were chosen as graph theory parameters to characterize local and global connectivity patterns, since they have been suggested to appropriately represent post-lesional alterations in network topology (Caliandro et al. 2017; Vecchio et al. 2019a, b). Connectivity indices and graph theoretical parameters were computed in theta (3–6 Hz), lower alpha (7–10 Hz), upper alpha (11–13 Hz) and beta (14–25 Hz) bands, to inspect a broad range of oscillations (Caliandro et. al. 2017). The lower and upper ranges of the alpha band were separately explored, to account for possible alterations in patients with posterior lesions, due to their previously documented slowdown in individual alpha frequency (Pietrelli et al. 2019). Finally, the relationship between visual performance in hemianopics and connectivity indices was also investigated, to explore whether specific connectivity alterations might be linked to visual impairments in hemianopics.

Materials and methods

Participants

Five groups of participants took part in the study: 14 patients (10 males, mean age = 53.08 years, SD = 15.32; mean education = 12.07 years, SD = 2.58; mean time since lesion onset = 12.64 months, SD = 11.59) with visual field defect due to lesions to the left posterior cortices, 13 patients with visual field defect due to lesions to the right posterior cortices (10 males, mean age = 58.9 years, SD = 16.47; mean education = 12 years, SD = 5.20; mean time since lesion onset = 12.47 months, SD = 14.18), a control group of nine patients without hemianopia with lesions to left fronto-temporal cortices, sparing the posterior cortices (5 males, mean age = 43.22 years, SD = 9.65; mean education = 14.67 years, SD = 2.69; mean time since lesion onset = 19.56 months, SD = 14.83), a control group of nine patients without hemianopia with lesions to right fronto-temporal cortices, sparing the posterior cortices (4 males, mean age = 51.67 years, SD = 9.97; mean education = 10.44 years, SD = 3.98; mean time since lesion onset = 23 months, SD = 25.15) and a control group of fourteen age-matched healthy participants (7 males, mean age 54.29 years, SD = 8.28; mean education = 13.28 years, SD = 3.12). No differences between the groups were found in terms of age ($F_{1,54}$ = 2.12; p = 0.091), education ($F_{1,54}$ = 1.761, p = 0.150) or time since lesion onset ($F_{1,41}$ = 1.072; p = 0.371; for clinical details, please see Table 1).

Table 1 Summary of demographic and clinical data of all patients that took part to the study

Subject	Sex	Age	Education	Onset	Lesion site	Visual field defect	Aetiology
HEMI L-LES 1	M	69	11	5	Left-occipital	Right hemianopia	Ischaemic
HEMI L-LES 2	M	45	13	7	Left-temporal	Right hemianopia	Hemorragic
HEMI L-LES 3	F	57	13	28	Left fronto-temporo-insular	Right hemianopia	AVM
HEMI L-LES 4	M	50	13	7	Left temporo-occipito-parietal	Upper right quadrantopia	Ischaemic
HEMI L-LES 5	M	81	5	9	Left occipito-temporal	Right hemianopia	Abscess
HEMI L-LES 6	M	51	13	5	Left fronto-temporo-occipital	Right hemianopia	Ischaemic
HEMI L-LES 7	M	41	13	2	Left occipital	Lower right quadrantopia	Hemorragic
HEMI L-LES 8	M	45	13	42	Left fronto-parieto-temporal	Right hemianopia	AVM
HEMI L-LES 9	F	29	15	26	Left temporal	Upper right quadrantopia	Ischaemic
HEMI L-LES 10	M	58	8	6	Left temporo-occipital	Right hemianopia	Ischaemic
HEMI L-LES 11	F	32	16	4	Left parieto-occipital	Right hemianopia	Ischaemic
HEMI L-LES 12	M	69	13	8	Left temporo-occipital	Right hemianopia	Hemorragic
HEMI L-LES 13	M	73	12	17	Left temporo-occipital	Right hemianopia	Hemorragic
HEMI L-LES 14	F	59	11	11	Left-mesial-temporal	Right hemianopia	AVM
HEMI R-LES 1	M	56	18	3	Right occipital	Left hemianopia	Ischaemic
HEMI R-LES 2	F	38	18	13	Right parieto-occipital	Left hemianopia	Hemorragic
HEMI R-LES 3	F	37	13	4	Right occipito-temporo-parietal	Left hemianopia	Tumor
HEMI R-LES 4	M	58	8	18	Right temporo-occipital	Left hemianopia	Ischaemic
HEMI R-LES 5	M	81	8	7	Right occipital	Left hemianopia	Hemorragic
HEMI R-LES 6	M	51	8	4	Right occipital	Left hemianopia	Tumor
HEMI R-LES 7	M	60	18	29	Right temporo-occipital	Left hemianopia	Ischaemic
HEMI R-LES 8	F	73	5	8	Right temporo-occipital	Left hemianopia	Ischaemic
HEMI R-LES 9	M	77	8	6	Right fronto-parietal	Left hemianopia	Hemorragic
HEMI R-LES 10	M	30	16	54	Right-temporal	Left hemianopia	Hemorragic
HEMI R-LES 11	M	59	18	5	Right temporo-occipital	Left hemianopia	Ischaemic
HEMI R-LES 12	M	76	13	7	Right temporo-occipital	Left hemianopia	Abscess
HEMI R-LES 13	M	70	18	5	Right occipital	Left hemianopia	Ischaemic
CONT L-LES 1	F	48	13	38	Left fronto-insular	No hemianopia	Ischaemic
CONT L-LES 2	F	44	13	40	Left frontal	No hemianopia	Tumor
CONT L-LES 3	M	28	18	11	Left fronto-parietal	No hemianopia	Tumor
CONT L-LES 4	F	45	11	39	Left frontal	No hemianopia	Tumor
CONT L-LES 5	F	46	15	12	Left temporal pole	No hemianopia	Hemorragic
CONT L-LES 6	M	62	18	7	Left temporo-insular	No hemianopia	Abscess
CONT L-LES 7	M	34	13	7	Left frontal	No hemianopia	Tumor
CONT L-LES 8	M	45	13	15	Left-frontal	No hemianopia	Ischaemic
CONT L-LES 9	F	37	13	7	Left frontal	No hemianopia	Tumor
CONT R-LES 1	F	57	13	5	Right fronto-insular	No hemianopia	AVM
CONT R-LES 2	M	42	18	59	Right frontal	No hemianopia	Abscess
CONT R-LES 3	F	42	11	19	Right frontal	No hemianopia	Tumor
CONT R-LES 4	M	51	8	3	Right temporo-insular	No hemianopia	Tumor
CONT R-LES 5	F	51	10	5	Right temporal	No hemianopia	Tumor
CONT R-LES 6	F	50	5	71	Right temporo-fronto-polar	No hemianopia	Traumatic
CONT R-LES 7	M	75	8	26	Right temporo-insular	No hemianopia	Tumor
CONT R-LES 8	F	46	8	13	Right-frontal	No hemianopia	Abscess
CONT R-LES 9	M	51	13	6	Right-frontal	No hemianopia	Tumor

Details about age and education are reported in years; details about onset of brain lesion are reported in months

M Male, *F* Female, *AVM* Arteriovenus malformation

Mapping of brain lesions was performed using MRIcro. Lesions documented by the most recent clinical CT or MRI were traced onto the T1-weighted MRI template from the Montreal Neurological Institute provided with MRIcro software (Rorden et al. 2007; Rorden and Brett 2000), with the exception of HEMI L-LES 7 and HEMI R-LES 8 whose MRI/CT scans were not available. Although lesion reconstruction was not performed for these two patients, radiology MRI/CT reports were available and confirmed the presence of unilateral lesions limited to the posterior cortices. Lesion volumes were computed for each patient in order to compare the extension of the lesions among the four patients' groups. No significant differences (one-way ANOVA, $F_{1,39} = 1.61$; $p = 0.201$) in lesion volumes between the four groups of patients were found (see Fig. 1). Patients with posterior lesions were recruited based on reported visual field defects, the availability of a visual field perimetry and CT/MRI reports of the lesion. In patients with posterior right lesions, the presence of neglect was screened using the Behavioral Inattention Test (Wilson et al. 1987), to ensure performance was in the normal range.

All patients showed normal or corrected-to-normal visual acuity. Patients were informed about the procedure and the purpose of the study and gave written informed consent. The study was designed and performed in accordance with the ethical principles of the Declaration of Helsinki and was approved by the Ethics Committee of the Regional Health Service Romagna (CEROM; n.2300).

EEG recordings

Participants comfortably seated in a soundproof room, while EEG signal was recorded from five sessions of one minute each, in an eyes-closed resting state condition. EEG data were acquired through a BrainAmp DC amplifier (BrainProducts GmbH, Germany) and Ag/AgCl electrodes (Fast'nEasy Cap, Easycap GmbH, Germany) from 59 scalp sites (Fp1, AF3, AF7, F1, F3, F7, FC1, FC3, FC5, FT7, C1, C3, C5, T7, CP1, CP3, CP5, TP7, P1, P3, P5, P7, PO3, PO7, O1, Fp2, AF4, AF8, F2, F4, F8, FC2, FC4, FC6, FT8, C2, C4, C6, T8, CP2, CP4, CP6, TP8, P2, P4, P6, P8, PO4, PO8, O2, FPz, AFz, Fz, FCz, Cz, CPz, Pz, POz, Oz) and the right mastoid. As online reference, the left mastoid electrode was used, while the ground electrode was placed on the right cheek. Vertical and horizontal electrooculogram (EOG) components were recorded from above and below the left eye, and from the outer canthus of each eye. Data were recorded with a band-pass filter of 0.01–100 Hz and digitized at a sampling rate of 1000 Hz, while impendences were kept under 5 KΩ.

EEG preprocessing

EEG recordings were processed off-line using EEGlab (v14.1.2; Delorme and Makeig 2004) and custom scripts developed in Matlab (R2018a; The Mathworks Inc., USA). Data from all electrodes were re-referenced to the average of all scalp electrodes and filtered with a band-pass filter of 1–100 Hz. Continuous signals were segmented in epochs of 1 s. Horizontal and vertical eye artifacts were visually identified and corrected with an independent component analysis (ICA), after data dimension reduction by means of Principal Component Analysis (PCA). Data were down-sampled to 250 Hz and current source density (CSD) interpolation, using spherical splines (Kayser and Tenke 2015) was applied to minimize confounding effects in inter-electrode synchronization due to volume conduction and field spread (van Diessen et al. 2015; Cohen 2014). CSD transformation was performed in Matlab using the open-source CSD toolbox (version 1.1; http://psychophysiology.cpmc.columbia.edu/Software/CSDtoolbox/).

Functional connectivity analysis

A multi-step approach was used to investigate, separately for each frequency band and hemisphere, the effects of

Fig. 1 Location and overlap of brain lesions of patients. The image shows the lesions of the hemianopic patients with left posterior brain lesion (**A**), hemianopic patients with right posterior brain lesion (**B**), control patients with left anterior brain lesion (**C**), control patients with right anterior brain lesion (**D**), projected onto four axial slices of the standard MNI brain. The levels of the axial slices are marked by white lines on the sagittal view of the brain. The color bar indicates the number of overlapping lesions

unilateral posterior or anterior brain lesions on functional connectivity and resting-state network topology.

Weighted phase-lag index

Functional connectivity was measured computing the weighted phase-lag index (wPLI, Vinck et al. 2011), which extends the phase-lag index (PLI, Stam et al. 2007) by weighting the contribution of observed phase leads and lags by the magnitude of the imaginary component of the cross-spectrum (Vinck et al. 2011). The wPLI is based on a consistent lag between the instantaneous phases of two electrodes and is less sensitive to zero-lag phase-relations typical for common sources (Bastos and Schoffelen 2016; Hardmeier et al. 2014).

To compute the wPLI, frequency decomposition was performed for all EEG channels, using a multitaper method with digital prolate spheroidal sequence (DPSS) windows, implemented in Fieldtrip toolbox (v20210311) for EEG/MEG-analysis (for the details of the implementations, see Vinck et al. 2011).

Complex Fourier coefficients were extracted for the frequency bands of interest, specifically in the theta (3–6 Hz), low alpha (7–10 Hz), upper alpha (11–13 Hz) and beta (14–25 Hz) ranges and 59×59 connectivity matrix was constructed for each participant and frequency band of interest. Then, the wPLIs computed for all possible pairs of electrodes within the left (Fp1, AF3, AF7, F1, F3, F7, FC1, FC3, FC5, FT7, C1, C3, C5, T7, CP1, CP3, CP5, TP7, P1, P3, P5, P7, PO3, PO7, O1) and the right (Fp2, AF4, AF8, F2, F4, F8, FC2, FC4, FC6, FT8, C2, C4, C6, T8, CP2, CP4, CP6, TP8, P2, P4, P6, P8, PO4, PO8, O2) hemisphere were averaged across pairs of electrodes and participants, to obtain an index of intrahemispheric functional connectivity. Electrodes on the sagittal midline were excluded from the analysis, to provide a better segregation of the signal of the two hemispheres. Finally, the wPLIs computed for all possible pairs of electrodes between the left and the right hemisphere were averaged across pairs of electrodes and participants, to obtain an index of interhemispheric functional connectivity. Electrodes on the sagittal midline were excluded from the analysis, to provide a better segregation of the signal between the left and the right hemisphere.

Intrahemispheric functional connectivity was compared among groups and hemispheres, separately for each frequency band (i.e., theta, lower alpha, upper alpha, beta), with an ANOVA on mean intrahemispheric wPLI having *Group* (Healthy participants, Left-lesioned hemianopic patients, Right-lesioned hemianopic patients, Left-lesioned control patients, Right-lesioned control patients) as between-subjects factor, and *Hemisphere* (Left, Right) as within-subjects factor. Last, to test for differences among groups in interhemispheric functional connectivity separately for

each frequency band (i.e. theta, lower alpha, upper alpha, beta), an ANOVA on mean interhemispheric wPLI having *Group* (Healthy participants, Left-lesioned hemianopic patients, Right-lesioned hemianopic patients, Left-lesioned control patients, Right-lesioned control patients) as between-subjects factor was run. Statistically significant interactions or main effects were subsequently explored through simple planned contrasts, comparing connectivity in each group of patients against connectivity in the group of Healthy participants.

Graph theory

Two graph theory measures, the clustering coefficient (C) and the characteristic path length (L), were chosen to assess the functional network segregation and integration, respectively. In particular, the C represents the degree to which nodes in a graph are interconnected whereas the L reflects the average shortest path length between all pairs of nodes in the network (Watts and Strogatz 1998). Graph indices were computed with custom scripts developed in Matlab, through the Brain Connectivity Toolbox (v1.1, Rubinov and Sporns 2010). Specifically, the C and the L were calculated separately for each band of interest (i.e., theta, low alpha, upper alpha, beta), on undirected weighted network matrices without thresholding, putting wPLI values as the edge weights.

The C (Onnela, et al. 2005) was defined as:

$$C^w = \frac{1}{n} \sum_{i \in N} \frac{2t_i^w}{k_i(k_i - 1)}$$

where C is the clustering coefficient of a given node (for details, see Rubinov and Sporns 2010).

The L (Runinov and Sporns, 2010) was defined as:

$$L^w = \frac{1}{n} \sum_{i \in N} \frac{\sum_{j \in N, j \neq i} d_{ij}^w}{n - 1}$$

where L is the average distance between a given node and all other nodes (for details, see Rubinov and Sporns 2010).

To test for differences in the functional integration and segregation within the two brain hemispheres, the C and the L parameters were separately computed for the left and the right hemisphere and averaged across participants. Electrodes on the sagittal midline were excluded from the analysis, to provide a better segregation of the signal of the two hemispheres. Then, possible differences among groups and hemispheres were tested separately for each frequency band (i.e. theta, low alpha, upper alpha, beta) with an ANOVA having *Group* (Healthy participants, Left-lesioned hemianopic patients, Right-lesioned hemianopic patients, Left-lesioned control patients, Right-lesioned control patients) as between-subjects factor, and *Hemisphere* (Left, Right) as

within-subjects factor. Statistically significant main effects or interactions were subsequently explored through simple planned contrasts, by comparing the mean C and L of each group of patients against the group of Healthy participants.

Computerized visual field test

In addition to the EEG recording, hemianopic patients' visual detection abilities were also tested (Làdavas et al. 2020; Grasso et al. 2016; Dundon et al. 2015a, b; Passamonti et al. 2009; Bolognini et al. 2005) during the clinical examination, to explore a possible link between visual performance and functional connectivity. Patients sat at a viewing distance of 120 cm, while a stimulus array of $52° \times 45°$ (horizontally and vertically, respectively) was projected on the wall. Targets, consisting of white dots ($1°$) were presented on a black background for 100 ms, at random positions. A red fixation cross ($0.5°$) was displayed on the center of the screen. A total of 96 targets was presented (i.e., 48 targets for each hemifield). In 31 trials, no target was presented (i.e., catch trials). Patients were instructed to press a response button after the detection of the target. Patients' gaze was monitored throughout the task by the experimenter. The task was performed in two different conditions: when patients were not allowed to move their eyes to compensate for the visual field loss and had to keep their gaze on a central fixation cross (Fixed-eyes) and when patients were allowed to perform eye movements (Eye movements). Visual detections and false alarms rates for stimuli presented in the blind visual field were measured. D prime (perceptual sensitivity) was calculated and used for subsequent correlational statistical analysis with the patients' wPLI and Graph theory indices that resulted to be impaired, compared to healthy participants.

Results

Functional connectivity in the theta band

Intrahemispheric wPLI

The ANOVA showed a significant main effect of *Group* ($F_{4,54} = 5.185$, $p = 0.001$, $\eta_p^2 = 0.277$), whereas the main effect of *Hemisphere* ($F_{1,54} = 0.001$, $p = 0.977$, $\eta_p^2 < 0.001$) was not significant. Importantly, the ANOVA showed also a significant *Group* $\times$ *Hemisphere* ($F_{4,54} = 2.879$, $p = 0.031$, $\eta_p^2 = 0.176$; see Fig. 2C) interaction, which was further explored through simple planned contrasts. More specifically, the intrahemispheric theta wPLI of each group of patients was contrasted against the group of healthy participants, separately for the left and the right hemisphere.

Planned contrast performed on the group of Left-lesioned hemianopics *vs* Healthy participants revealed no

significant difference between the two groups in the left hemisphere (Left-lesioned hemianopics η_p^2 0.19, Healthy participants $M = 0.18$; $p = 0.776$) nor in the right hemisphere (Left-lesioned hemianopics $M = 0.17$, Healthy participants $M = 0.16$; $p = 0.743$). Similarly, planned contrast on the group of Right-lesioned hemianopics vs Healthy participants did not show a significant difference in the left hemisphere (Right-lesioned hemianopics $M = 0.21$; $p = 0.141$). However, Right-lesioned hemianopics exhibited a significantly increased wPLI in the right hemisphere ($M = 0.25$), compared to the right hemisphere of healthy participants ($p < 0.001$). Last, planned contrast on the group of both Right-lesioned and Left-lesioned control patients *vs* Healthy participants revealed no significant difference neither in the left (all ps > 0.057) or in the right (all ps > 0.314) hemisphere.

Clustering coefficient

The ANOVA revealed a significant main effect of *Group* ($F_{4,54} = 5.249$, $p = 0.001$, $\eta_p^2 = 0.280$), whereas the main effect of *Hemisphere* ($F_{1,54} = 0.005$, $p = 0.943$, $\eta_p^2 < 0.001$) was not significant. Importantly, the ANOVA showed also a significant *Group* $\times$ *Hemisphere* ($F_{4,54} = 2.591$, $p = 0.047$, $\eta_p^2 = 0.161$; see Fig. 2D) interaction, which was further explored by performing planned contrast.

Planned contrast performed on the group of Left-lesioned hemianopics against the group of Healthy participants did not show any significant difference neither in the left (Left-lesioned hemianopics $M = 0.17$, Healthy participants $M = 0.17$, $p = 0.754$) or in the right (Left-lesioned hemianopics $M = 0.16$, Healthy participants $M = 0.17$, $p = 0.698$) hemisphere. Planned contrast on the group of Right-lesioned hemianopics *vs* Healthy participants revealed no significant difference in the left hemisphere (Right-lesioned hemianopics $M = 0.20$, $p = 0.132$) but, importantly, Right-lesioned hemianopics exhibited a higher theta C in the right hemisphere, compared to the right hemisphere of Healthy participants (Right-lesioned hemianopics $M = 0.22$, $p < 0.001$).

Last, for both groups of Left-lesioned and Right-lesioned control patients, planned contrast performed against Healthy participants showed no significant difference in the left hemisphere (all ps > 0.057) nor in the right hemisphere (all ps > 0.316).

Characteristic path length

The ANOVA showed no significant main effect of *Hemisphere* ($F_{1,54} = 0.657$, $p = 0.421$, $\eta_p^2 = 0.012$), nor a significant *Group* $\times$ *Hemisphere* interaction ($F_{4,54} = 1.036$, $p = 0.397$, $\eta_p^2 = 0.071$), but a significant main effect of *Group* ($F_{4,54} = 4.445$, $p = 0.004$, $\eta_p^2 = 0.248$; see Fig. 2E).
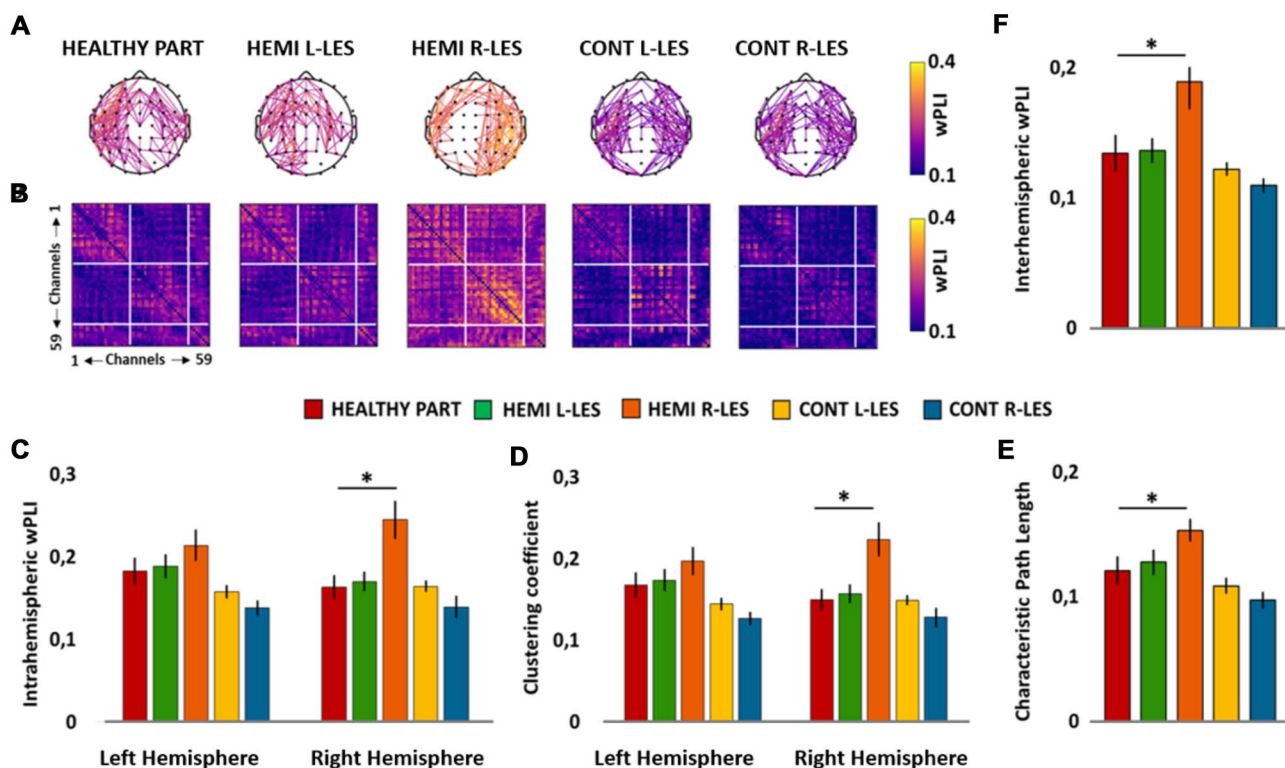
Fig. 2 Scalp maps **A** represent the strongest theta connections ($n = 171$, 10% of total connections) in the group of healthy participants (HEALTHY PART), hemianopic patients with left lesion (HEMI L-LES), hemianopic patients with right lesion (HEMI R-LES), control patients with left anterior lesion (CONT L-LES) and control patients with right anterior lesion (CONT R-LES) The color bar represents the wPLI value, so that higher values are associated with yellow color and lower values with blue color. Panel **B** represents the theta band functional connectivity matrices of the wPLIs calculated for each of the five groups. Bar histograms show the mean theta (3–6 Hz) intrahemispheric wPLI relative to the left and to the right hemisphere, within each group (**C**), the mean theta clustering coefficient relative to the left and to the right hemisphere, within each group (**D**), the mean theta characteristic path length within each group (**E**) and the mean theta interhemispheric wPLI within each group (**F**). Error bars represent standard error; asterisks indicate the significant comparisons

Importantly, planned contrast revealed a significantly greater theta L for the group of Right-lesioned hemianopics ($M = 0.15$) compared to Healthy participants ($M = 0.12$, $p = 0.015$), whereas no other significant difference was found (all ps > 0.106).

Interhemispheric wPLI

The ANOVA on the interhemispheric wPLI in the theta band showed a significant main effect of *Group* ($F_{4,54} = 4.638$, $p = 0.003$, $\eta_p^2 = 0.256$; see Fig. 2F). Planned contrasts comparing the theta interhemispheric wPLI of each group of patients against the group of healthy controls revealed a significantly higher interhemispheric wPLI for the group of Right-lesioned hemianopics ($M = 0.19$), compared to healthy participants ($p = 0.005$). No other significant difference was found (all ps > 0.235).

Functional connectivity in the lower alpha band

Intrahemispheric wPLI

The ANOVA on the intrahemispheric wPLI in the lower alpha band did not show a significant main effect of *Group* ($F_{4,54} = 0.226$, $p = 0.923$, $\eta_p^2 = 0.016$), nor a significant effect of *Hemisphere* ($F_{1,54} = 1.134$, $p = 0.292$, $\eta_p^2 = 0.021$), but a significant *Group × Hemisphere* ($F_{4,54} = 3.162$, $p = 0.021$, $\eta_p^2 = 0.190$; see Fig. 3C) interaction. However, planned contrast performed on this significant interaction showed no significant differences for none of the groups of patients, compared to healthy participants, neither in the left (all ps > 0.408) nor in the right hemisphere (all ps > 0.349).
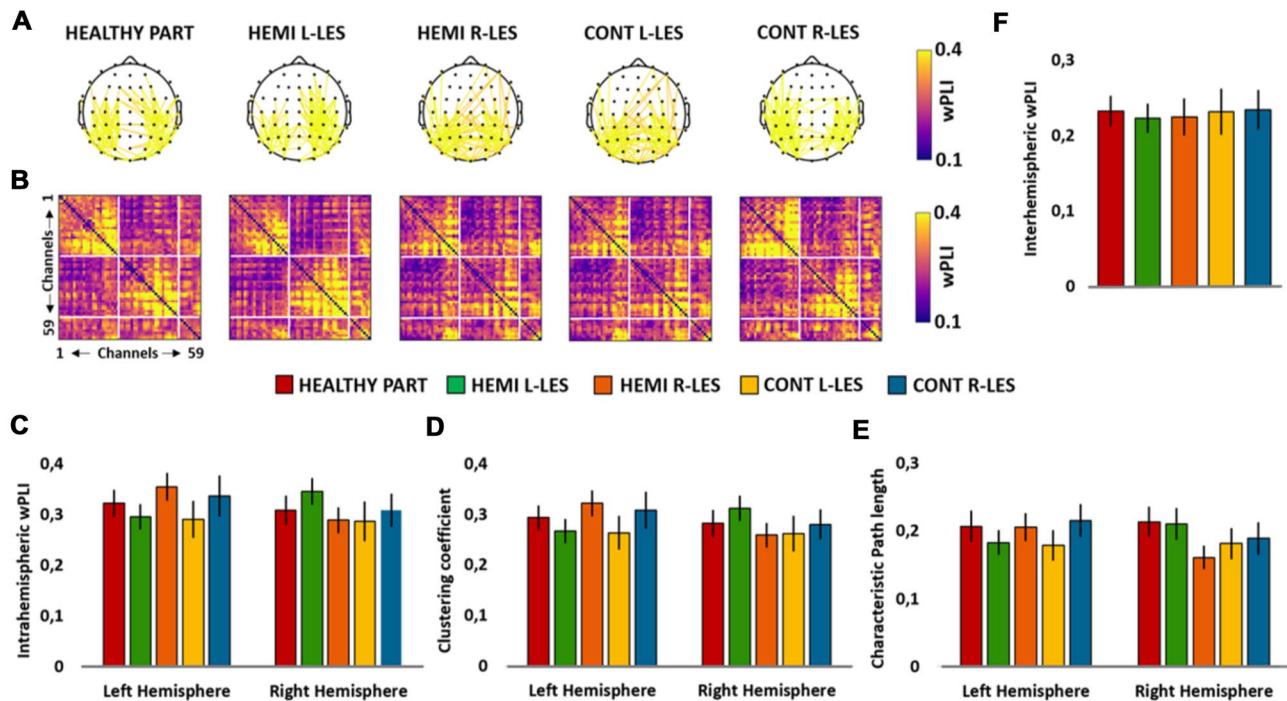
Fig. 3 Scalp maps **A** represent the strongest lower alpha connections ($n = 171$, 10% of total connections) in the group of healthy participants (HEALTHY PART), hemianopic patients with left lesion (HEMI L-LES), hemianopic patients with right lesion (HEMI R-LES), control patients with left anterior lesion (CONT L-LES) and control patients with right anterior lesion (CONT R-LES) The color bar represents the wPLI value, so that higher values are associated with yellow color and lower values with blue color. Panel **B** represents the lower alpha band functional connectivity matrices of the wPLIs calculated for each of the five groups. Bar histograms show the mean lower alpha (7–10 Hz) intrahemispheric wPLI relative to the left and to the right hemisphere, within each group (**C**), the mean lower alpha clustering coefficient relative to the left and to the right hemisphere, within each group (**D**), the mean lower alpha characteristic path length relative to the left and to the right hemisphere, within each group (**E**), the mean lower alpha interhemispheric wPLI within each group (**F**). Error bars represent standard error; asterisks indicate the significant comparisons

Clustering coefficient

The ANOVA on the low alpha C did not reveal a significant main effect of *Group* ($F_{4,54} = 0.204$, $p = 0.935$, $\eta_p^2 = 0.015$), nor a significant main effect of *Hemisphere* ($F_{1,54} = 1.247$, $p = 0.269$, $\eta_p^2 = 0.023$), but a significant *Group × Hemisphere* ($F_{4,54} = 3.266$, $p = 0.019$, $\eta_p^2 = 0.193$; see Fig. 3D) interaction.

However, planned contrast showed no significant differences for none of the groups of patients, compared to healthy participants, neither in the left (all ps > 0.443) or in the right hemisphere (all ps > 0.416).

Characteristic path length

The ANOVA revealed no significant main effect of *Group* ($F_{4,54} = 0.436$, $p = 0.782$, $\eta_p^2 = 0.031$) and *Hemisphere* ($F_{1,54} = 0.493$, $p = 0.486$, $\eta_p^2 = 0.009$), nor a significant *Group × Hemisphere* interaction ($F_{4,54} = 1.903$, $p = 0.123$, $\eta_p^2 = 0.124$; see Fig. 3E).

Interhemispheric wPLI

Last, the ANOVA performed on the interhemispheric wPLI in the low alpha band did not reveal a significant main effect of *Group* ($F_{4,54} = 0.048$, $p = 0.996$, $\eta_p^2 = 0.004$; see Fig. 3F).

Functional connectivity in the upper alpha band

Intrahemispheric wPLI

For the upper alpha band, the ANOVA on the intrahemispheric wPLI did not reveal a significant main effect of *Group* ($F_{4,54} = 1.791$, $p = 0.144$, $\eta_p^2 = 0.017$), nor a significant main effect of *Hemisphere* ($F_{1,54} = 2.129$, $p = 0.150$, $\eta_p^2 = 0.038$) but, importantly, the ANOVA showed a significant *Group × Hemisphere* ($F_{4,54} = 2.787$, $p = 0.035$, $\eta_p^2 = 0.171$; see Fig. 4C) interaction.

Planned contrast performed on the group of Left-lesioned hemianopics *vs* Healthy participants revealed a significantly decreased wPLI in the left hemisphere of Left-lesioned hemianopics ($M = 0.24$), compared to the left hemisphere
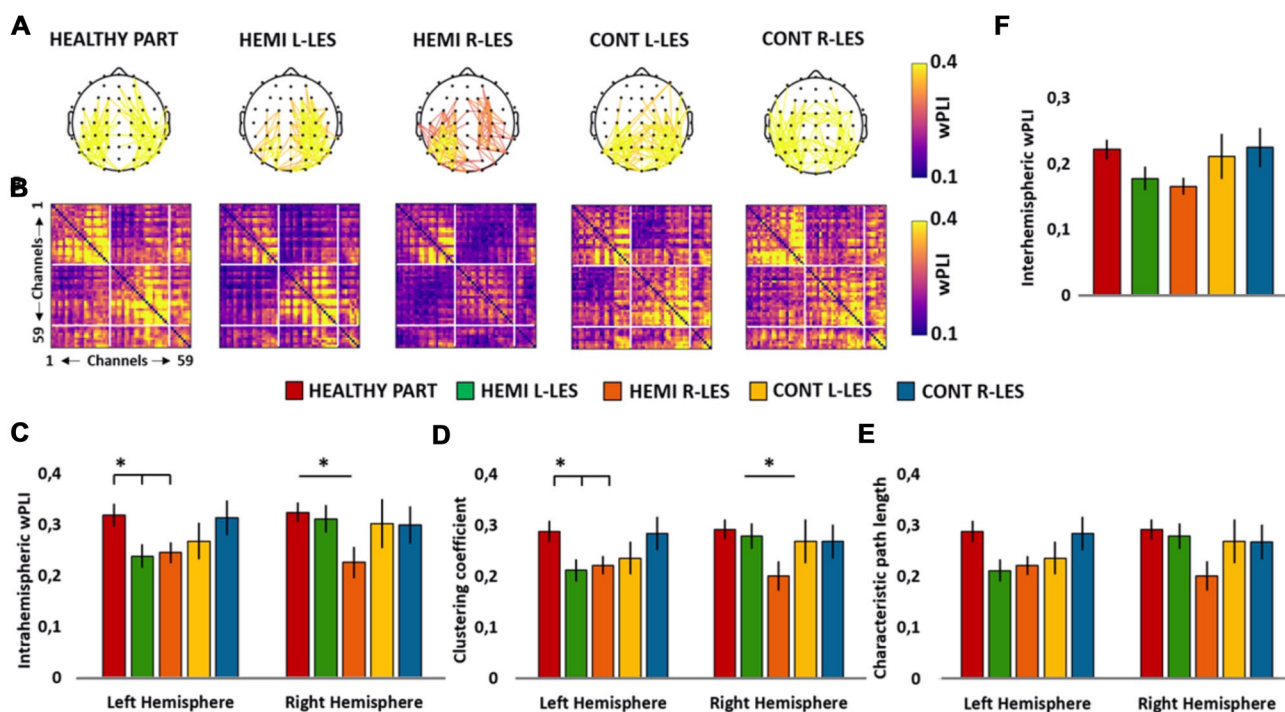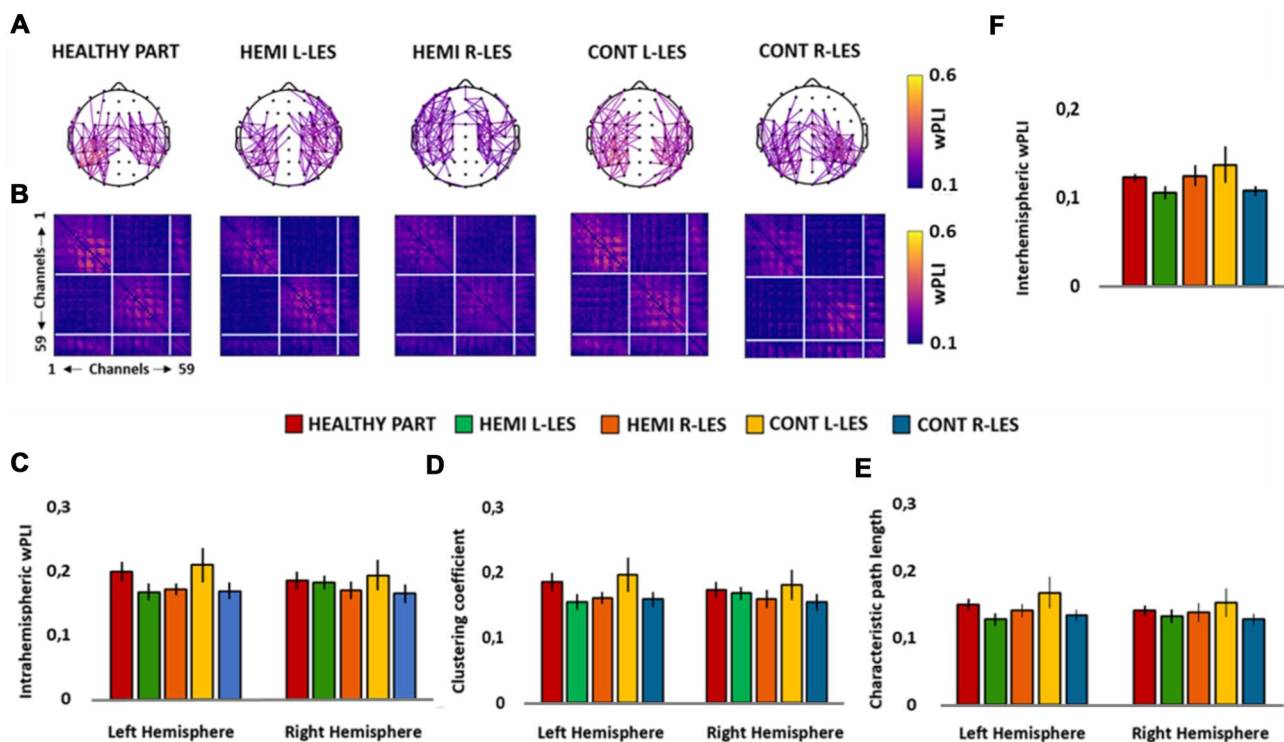
Fig. 4 Scalp maps **A** represent the strongest upper alpha connections ($n = 171$, 10% of total connections) in the group of healthy participants (HEALTHY PART) hemianopic patients with left lesion (HEMI L-LES), hemianopic patients with right lesion (HEMI R-LES), control patients with left anterior lesion (CONT L-LES) and control patients with right anterior lesion (CONT R-LES) The color bar represents the wPLI value, so that higher values are associated with yellow color and lower values with blue color. Panel **B** represents the upper alpha band functional connectivity matrices of the wPLIs calculated for each of the five groups. Bar histograms show the mean upper alpha (11–13 Hz) intrahemispheric wPLI relative to the left and to the right hemisphere, within each group (**C**), the mean upper alpha clustering coefficient relative to the left and to the right hemisphere, within each group (**D**), the mean upper alpha characteristic path length relative to the left and to the right hemisphere, within each group (**E**) and the mean upper alpha interhemispheric wPLI within each group (**F**). Error bars represent standard error; asterisks indicate the significant comparisons

of Healthy participant ($M = 0.32$, $p = 0.020$), whereas no significant difference between the two groups was found in the right hemisphere (Left-lesioned hemianopics $M = 0.31$, Healthy participants $M = 0.32$, $p = 0.749$). For the group of Right-lesioned hemianopics, planned contrasts revealed a significant decrease in wPLI both in the left ($M = 0.25$; $p = 0.036$) and in the right ($M = 0.22$; $p = 0.019$) hemisphere, compared to healthy participants. Last, for both groups of Left-lesioned and Right-lesioned control patients, planned contrast against Healthy participants revealed no significant difference neither in the left (all ps > 0.186), nor in the right hemisphere (all ps > 0.582).

Clustering coefficient

The ANOVA on the C in the upper alpha band did not show a significant main effect of *Group* ($F_{4,54} = 1.749$, $p = 0.153$, $\eta_p^2 = 0.115$), nor a significant main effect of *Hemisphere* ($F_{1,54} = 1.757$, $p = 0.191$, $\eta_p^2 = 0.032$), but a significant *Group × Hemisphere* ($F_{4,54} = 2.958$, $p = 0.028$, $\eta_p^2 = 0.180$, see Fig. 4D) interaction.

Planned contrast on Left-lesioned hemianopics *vs* Healthy participants revealed a significantly lower C in the left hemisphere of Left-lesioned hemianopics ($M = 0.21$), compared to the left hemisphere of Healthy participants ($M = 0.29$, $p = 0.017$), whereas no significant difference between the two groups was found for the right hemisphere (Left-lesioned hemianopics $M = 0.28$, Healthy participants $M = 0.29$; $p = 0.727$). Similarly, also for the group of Right-lesioned hemianopics, planned contrasted revealed a significantly lower C in the left hemisphere ($M = 0.22$), compared to the left hemisphere of healthy participants ($p = 0.041$). Furthermore, Right-lesioned hemianopics exhibited also a lower C in the right hemisphere ($M = 0.20$), compared to the right hemisphere of Healthy participants ($p = 0.020$). In contrast, for both groups of Left-lesioned and Right-lesioned control patients, no significant comparison was found in the left hemisphere (all ps > 0.142), nor in the right hemisphere (all ps > 0.573), relative to Healthy participants.

Characteristic path length

The ANOVA revealed no significant main effect of *Group* ($F_{4,54} = 2.210$, $p = 0.080$, $\eta_p^2 = 0.141$) and *Hemisphere* ($F_{1,54} = 0.486$, $p = 0.489$, $\eta_p^2 = 0.09$), nor a significant *Group* × *Hemisphere* interaction ($F_{4,54} = 2.079$, $p = 0.096$, $\eta_p^2 = 0.133$; see Fig. 4E).

Interhemispheric wPLI

Last, the ANOVA performed on the upper alpha interhemispheric wPLI did not show a significant main effect of *Group* ($F_{4,54} = 1.748$, $p = 0.153$, $\eta_p^2 = 0.115$, see Fig. 4F).

Functional connectivity in the beta band

Intrahemispheric wPLI

The ANOVA performed on the intrahemispheric wPLI in the beta band revealed no significant main effect of

Group ($F_{4,54} = 0.984$, $p = 0.423$, $\eta_p^2 = 0.105$), nor a significant main effect of *Hemisphere* ($F_{1,54} = 0.593$, $p = 0.444$, $\eta_p^2 = 0.053$). In addition, the ANOVA showed no significant *Group* × *Hemisphere* ($F_{4,54} = 1.180$, $p = 0.329$, $\eta_p^2 = 0.100$; see Fig. 5C) interaction.

Clustering coefficient

The ANOVA performed on the C in the beta band showed no significant main effect of *Group* ($F_{4,54} = 0.979$, $p = 0.426$, $\eta_p^2 = 0.108$), or *Hemisphere* ($F_{1,54} = 0.593$, $p = 0.444$, $\eta_p^2 = 0.032$), nor a significant *Group* × *Hemisphere* ($F_{4,54} = 2.958$, $p = 0.128$, $\eta_p^2 = 0.180$, see Fig. 5D) interaction.

Characteristic path length

The ANOVA did not reveal a significant main effect of *Group* ($F_{4,54} = 1.074$, $p = 0.378\ 0$, $\eta_p^2 = 0.112$) and

Fig. 5 Scalp maps **A** represent the strongest beta connections ($n = 171$, 10% of total connections) in the group of healthy participants (HEALTHY PART) hemianopic patients with left lesion (HEMI L-LES), hemianopic patients with right lesion (HEMI R-LES), control patients with left anterior lesion (CONT L-LES) and control patients with right anterior lesion (CONT R-LES) The color bar represents the wPLI value, so that higher values are associated with yellow color and lower values with blue color. Panel **B** represents the beta band functional connectivity matrices of the wPLIs calculated for each of the five groups. Bar histograms show the mean beta (14–25 Hz) intrahemispheric wPLI relative to the left and to the right hemisphere, within each group **(C)**, the mean beta clustering coefficient relative to the left and to the right hemisphere, within each group **(D)**, the mean beta Characteristic path length relative to the left and to the right hemisphere, within each group **(E)** and the mean beta interhemispheric wPLI within each group **(F)**. Error bars represent standard error; asterisks indicate the significant comparisons

Hemisphere ($F_{1,54} = 0.590$, $p = 0.212$, $\eta_p^2 = 0.105$). Also the *Group* × *Hemisphere* interaction ($F_{4,54} = 1.645$, $p = 0.622$, $\eta_p^2 = 0.009$; see Fig. 5E) was not significant.

Interhemispheric wPLI

Also, the ANOVA on the beta interhemispheric wPLI showed no significant main effect of *Group* ($F_{4,54} = 1.252$, $p = 0.298$, $\eta_p^2 = 0.088$, see Fig. 5F).

Hemianopic patients' visual performance and functional connectivity

Finally, we tested whether altered theta and upper alpha functional connectivity can relate to behavioral performance in visual detection tests in hemianopic patients with both left and right lesions. To this aim, the relationship between hemianopic patients' perceptual sensitivity (D prime) in their blind field at the Computerized Visual Field test and their functional connectivity parameters that resulted to be impaired was explored. More specifically, hemianopic patients' D prime in both the Fixed-Eyes condition and in the Eye-Movements condition was correlated to the intrahemispheric wPLI, the C and the L in the theta band and to the intrahemispheric wPLI and the C in the upper alpha band, separately for the lesioned and the intact hemisphere and, last, to the interhemispheric wPLI in the theta band. Pearson correlations were performed (Bonferroni-Holm corrections were used for multiple comparisons; adjusted p-levels are reported).

In the Fixed-Eyes condition, no significant correlation between the theta intrahemispheric wPLI in both the lesioned and the intact hemisphere and the D prime was found (all ps = 0.100). Similarly, no significant correlation was found between visual performance and the theta C in both the lesioned and the intact hemisphere (all ps = 0.100) and visual performance and the theta L in the lesioned or the intact hemisphere (all ps = 0.100). Last, no significant correlation between interhemispheric theta wPLI and D prime in the blind visual field was found ($r = -0.351$, $p = 0.072$), therefore, suggesting no relationship between connectivity parameter in the theta range and visual detection performance in the blind visual field when eye movements were prevented.

As for the upper alpha range, no significant correlation between the intrahemispheric wPLI in the intact hemisphere and the D prime ($r = 0.225$, $p = 0.257$) was found, but, importantly, a positive significant correlation between the upper alpha intrahemispheric wPLI in the lesioned hemisphere and the D prime ($r = 0.496$, $p = 0.016$, see Fig. 6A) emerged (i.e., the higher the upper alpha intrahemispheric wPLI in the lesioned hemisphere, the better the performance in patients' blind field). In line, also a positive significant correlation between upper alpha C in the lesioned hemisphere and the D prime ($r = 0.541$, $p = 0.006$, see Fig. 6B) was found, suggesting that higher upper alpha C in the
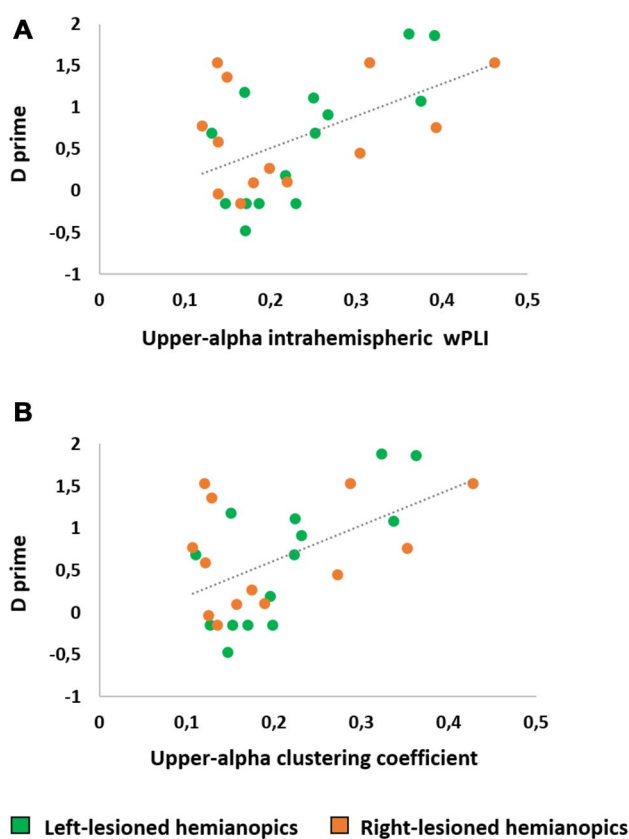

Fig. 6 Correlations between the hemianopic patients' visual performance in the Computerized Visual Field test in the Fixed-Eyes condition and functional connectivity parameters. Panel **A** depicts the correlation between D prime and upper alpha intrahemispheric wPLI; Panel **B** depicts the correlation between D prime and the upper alpha clustering coefficient

lesioned hemisphere is predictive of better performance in hemianopic patients' blind field. In contrast, no significant correlation between the upper alpha C in the intact hemisphere and the D prime was found ($r = 0.264$, $p = 0.182$). Overall, these findings indicate that upper alpha functional connectivity in the lesioned hemisphere in hemianopic patients is associated with visual detection performance in their blind visual field.

Finally, in the Eyes-Movements condition, no significant correlation with hemianopic patients' D prime in the blind field was found (all ps > 0.074), suggesting that both the theta and the upper alpha functional connectivity are not related to patients' ability to compensate for the field loss when eye movements are allowed.

Discussion

The present study has revealed that posterior brain lesions selectively impair oscillatory brain connectivity at rest. More precisely, both hemianopics with left and

right posterior lesions showed a reduction in intrahemispheric functional connectivity in the range of upper alpha (11–13 Hz) during resting state, while control patients with anterior lesions revealed no connectivity change compared to healthy individuals. Moreover, posterior right lesions seemed to induce more severe alterations in the oscillatory connectivity patterns, with hemianopics with right lesions showing a reduced intrahemispheric upper alpha connectivity in both the lesioned and the intact hemisphere and additional abnormal increase in connectivity in the theta range. On the contrary, left-lesioned hemianopics revealed only a reduction in intrahemispheric upper alpha connectivity limited to the lesioned hemisphere.

These results are in line with previous literature documenting dysfunctions in connectivity patterns after brain damage (Dubovik et al. 2012; Westlake et al. 2012; Wu et al. 2011; Castellanos et al. 2010; Guiggisberg et al. 2008) but also add to previous knowledge that lesions to posterior cortices, damaging the crucial hub for the generation and distribution of alpha oscillations, specifically impair connectivity in this frequency band. Accordingly, previous evidence on hemianopics revealed that posterior lesions impair oscillations in the alpha range, with a slowdown of the speed of processing in alpha (i.e., a reduction of alpha peak), the occurrence of an interhemispheric power imbalance, in favor of the intact hemisphere (Pietrelli et al. 2019) and a reduction of alpha reactivity induced by eyes-opening (Gallina et al. 2021). Therefore, as a whole, these findings corroborate the notion that alpha oscillatory patterns at rest can reflect the underlying functioning of the visual system, since lesions to posterior visual brain regions specifically impair activity in this frequency band. In line with this view, alpha oscillations represent the dominant frequency range of activity of the resting human brain and their distribution is prominent over posterior cerebral regions (Rosanova et al. 2009; Berger 1929). Accordingly, posterior visual cortices have been demonstrated to be crucial in generating and propagating alpha oscillations in the visual system (Hindriks et al. 2015; Bollimunta et al. 2008). In addition, oscillations in the alpha range are reportedly linked to visual perception and visual cortex activity (Romei et al. 2008a, 2008b; Pfurtscheller et al. 1994).

Hemianopic patients with posterior lesions showed connectivity impairments only in the upper range of the alpha band, consistently with previous evidence reporting, in these patients, a shift towards slower frequencies of the individual alpha peak (Pietrelli et al. 2019). Indeed, converging evidence have reported that occipito-parietal alpha generators, which might be impaired after posterior lesions, are more linked with oscillatory activity in the upper alpha band (Cantero et al. 2002). In line, the activity of the parieto-occipital oscillations in the upper alpha

range has been consistently linked with a greater efficiency of the visual processing, with the faster alpha frequencies being related to a more effective task execution both within (Zhang et al. 2019; Wutz et al. 2018; Minami and Amano 2017; Samaha and Postle 2015) and across (Venskus and Huighes 2021; Cooke et al. 2019; Cecere et al. 2015) sensory modalities.

Importantly, hemianopic patients with posterior lesions did not show altered patterns of functional connectivity in the beta range at rest, both intra- and inter-hemispheres. Altered oscillatory activity in the beta band has been reported in stroke patients in task-related oscillatory activity (Guggisberg et al. 2015) and also in hemianopics, mostly associated to impaired stimulus processing in visual and attentional tasks (Allaman et al. 2021; Sanchez-Lopez et al. 2020). However, the present findings suggest that, when looking at oscillatory patterns at rest, a damage to the posterior brain areas impair the functional connectivity patterns selectively in the range of alpha.

Relative to the role of alpha oscillatory activity in functional neural connectivity, long-range alpha synchronous activity has been shown to be relevant to promote communication between regions according to task demands (Doesburg et al. 2009; Palva and Palva 2007; Cooke et al. 2019) and coherent alpha oscillations seem to represent one of the main mechanisms of global resting-state integration in the human brain (Guggisberg et al. 2015). Accordingly, alpha cortico-cortical interactions have been suggested to reflect top-down processing, subserving the ability to integrate local bottom-up information (von Stein and Sarnthein 2000). Notably, post-lesional alterations in the alpha band were observed only in intrahemispheric connectivity in hemianopic patients, while alpha interhemispheric connectivity was similar between patients and healthy controls. In line with this finding, where functional connectivity is measured by wPLI, which is an index of lagged phase synchronization, previous evidence has suggested that post-stroke behavioral outcome can be predicted by phase-lagged alpha oscillations in intrahemispheric networks (Guggisberg et al. 2015). In contrast, interhemispheric interactions have shown to be predictive of post-lesional behavior, only when considering amplitude similarities with no phase lag in the beta (Guggisberg et al. 2015).

The present results also highlight the topological features of these post-lesional connectivity changes, showing that the reduced connectivity in upper alpha, is characterized by a decrease in local functional segregation (i.e., clustering coefficient), with no associated change in global functional integration (i.e., characteristic path length). Effective functional segregation has been reported to represent the ability of specific brain regions to integrate all the available information into complex specialized processes, through densely interconnected modules or clusters (Friston 2011). Moreover,

network efficiency has typically been described as a balance between this dense local clustering and short path length to integrate information from distant nodes (Sporns 2011; Bassett and Bullmore 2006). Therefore, the observed post-lesional changes in hemianopics suggest a disruption of the optimal brain functional structure, mainly due to a weakened local functional specialization. Previous reports on stroke patients at the acute stage have demonstrated post-lesional decrease in local alpha connectivity processing, which was compensated by a concurrent increase in distant functional integration, suggesting a rearrangement of alpha functional networks, due to plastic compensatory mechanisms occurring immediately after lesions (Caliandro et al. 2017). Following this reasoning, the present findings on hemianopic patients with posterior lesions at the chronic stage, showing an impairment in local alpha functional networks not associated with a concurrent a strengthening of global integration, might represent a signature of the topological dysfunction at the chronic stage after posterior lesions.

In keeping, our results also show a strong association between performance in clinical visual tests and connectivity patterns in the alpha range. Indeed, visual detection performance in the blind field, when eye movements were restricted (Grasso et al. 2016; Passamonti et al. 2009; Bolognini et al. 2005) was positively correlated with connectivity index and clustering coefficient in the upper alpha range. In contrast, no association between alpha connectivity and visual performance, when compensatory eye movements were allowed, was found. These findings suggest a strong link between alpha connectivity patterns after posterior lesions and the basic visual functioning of the visual system (i.e., the size of spared visual field), while more strategic, compensatory visual mechanisms seem not related to these connectivity measures. Accordingly, impaired pattern of alpha functional connectivity has also been observed in patients with visual loss due to pre-chiasmatic lesions (Bola et al. 2014) or retinal damage (Bola et al. 2015). These findings suggest that alterations in alpha functional connectivity during rest can be detrimental for visual performance and, therefore, might represent an index of impairment of the structural and functional integrity of the visual system, reflecting the presence of lesions in visual brain regions or peripheral damage.

Interestingly, right posterior lesions led to a more profound impairment in oscillatory functional connectivity. Indeed, while after left posterior lesions, reduction in intra-hemispheric alpha connectivity was found only in the hemisphere ipsilateral to the lesion, in case of lesions of the right posterior cortices the reduction in alpha intrahemispheric connectivity was bilaterally distributed all over the scalp. Moreover, the impairment in alpha connectivity after right posterior lesions was also associated to an abnormal increase in theta connectivity, both intra- and inter-hemispheres. These observations are reminiscent of previous findings

revealing at rest that hemianopics with right lesions showed a stronger alpha peak reduction and a more pronounced alpha power interhemispheric imbalance, compared to left-lesioned hemianopics (Pietrelli et al. 2019). Similarly, posterior right lesions also induced a more severe and distributed decrease in alpha reactivity at the opening of the eyes at rest, combined to a disruption in theta reactivity (Gallina et al. 2021).

The presence of more severe and distributed alterations in connectivity patterns in the right-lesioned hemianopic patients may raise the question of whether distinct post-lesional patterns of functional connectivity in the left-lesioned and in the right-lesioned hemianopics also reflect on different outcomes in visual performance. However, to disclose possible hemispheric differences in the patients' performance, a large sample of patients and specific and sensitive visual tasks, which are not available in the current investigation, are required. Therefore, future studies are needed to further explore differences in post-lesional visual performance depending on the side of the lesion.

Crucially, the more detrimental effects in oscillatory patterns after right posterior lesions seems to suggest a specialization of the right hemisphere in the generation and distribution of alpha oscillations, in line with previous studies consistently reporting a more pronounced alpha activity over the right posterior scalp sites at rest (Metzen et al. 2022). Accordingly, a dominance of the right hemisphere in modulating alpha oscillations, in order to allocate visuo-spatial attentional resources and tune visual perceptual abilities, has also been demonstrated during spatial orienting tasks with directional cues in healthy individuals (Gallotto et al. 2020).

Notably, although previous reports have documented post-lesional increased connectivity in low frequencies (delta-theta; Dubovik et al. 2012; Castellanos et al. 2010), the present findings seem to suggest that altered theta connectivity might be linked to specific lesional profiles, involving posterior cortices in the right hemisphere, and is consistently associated to impairments also in alpha connectivity. Moreover, graph theoretical analyses revealed that theta connectivity impairment is characterized by an increase in local segregated activity (i.e. increased clustering coefficient) and a decrease in global integration (i.e., higher path length), suggesting both a local and global inefficiency in theta activity. This suggests that a severe and bilateral reduction in alpha connectivity (as observed in right-damaged hemianopics) also induces impairments in local and global low-level processing in the theta range. In line, alpha oscillatory activity is thought to reflect widespread cortical networks' activity, regulating modular processes (Barry and De Blasio 2017; Doesburg et al. 2009) and orchestrating oscillatory activity in different frequency bands (Hindriks et al. 2015). In this perspective, we can speculate that in case of left posterior lesions, spared activity in the right intact hemisphere,

which shows normal alpha connectivity patterns, might be sufficient to preserve normal connectivity also in the theta range. On the contrary, right posterior lesions disrupt such oscillatory regulatory mechanisms, leading to functional connectivity impairments also in the theta range, therefore, suggesting that the right hemisphere might have a pivotal role in this mechanism. This seems in agreement with a longstanding range of evidence reporting a dominance of the right hemisphere in perceptual and visuo-spatial processing (Bueichekú et al. 2020; Corballis et al. 2002; Nicholls and Roberts 2002; Jewell and McCourt 2000; Gitelman et al. 1999; McCourt and Jewell 1999; McCourt and Olafson 1997; Nobre et al. 1997; Mattingley et al. 1994; Heilman et al. 1984; Heilman and Valenstein 1979; Bisiach and Luzzatti 1978) and corroborate the notion that oscillatory mechanisms might play a role in this specialized function.

Overall, the present results suggest that different lesional profiles might differentially alter functional connectivity and show that lesions to posterior cortices specifically impair functional connectivity in the alpha range. This suggests that the connectivity in the alpha range might represent an index of the integrity of the underlying visual system and supports the role of alpha oscillations in regulating local and global oscillatory patterns in lower frequency bands.

To conclude, there is accumulating evidence converging on the notion that the alpha oscillatory patterns at rest may represent a reliable signature of the functional and structural dynamics of the damaged visual system. Importantly, alpha oscillatory activity is known to be susceptible to functional changes and can be effectively modulated with external stimulations through various non-invasive brain techniques, such as transcranial magnetic stimulation (TMS), transcranial alternating current stimulation (tACS), rhythmic sensory entrainment methods or neurofeedback. This holds promise for future studies to develop effective therapeutic interventions for patients with posterior brain lesions, targeting alpha oscillatory power, frequency and functional connectivity at rest, to promote the functioning of the visual system and to ameliorate visual abilities in hemianopic patients (Dundon et al. 2015a, b).

Declarations

References

Achard S, Salvador R, Whitcher B, Suckling J, Bullmore E (2006) A resilient, low-frequency, small-world human brain functional network with highly connected association cortical hubs. J Neurosci 26(1):63–72. https://doi.org/10.1523/JNEUROSCI.3874-05.2006

Aertsen AM, Gerstein GL, Habib MK, Palm G (1989) Dynamics of neuronal firing correlation: modulation of "effective connectivity." J Neurophysiol 61(5):900–917. https://doi.org/10.1152/jn.1989.61.5.900

Allaman L, Mottaz A, Guggisberg AG (2021) Disrupted resting-state EEG alpha-band interactions as a novel marker for the severity of visual field deficits after brain lesion. Clin Neurophysiol 132(9):2101–2109. https://doi.org/10.1016/j.clinph.2021.05.029

Babiloni C, Frisoni GB, Pievani M, Vecchio F, Infarinato F, Geroldi C, Salinari S, Ferri R, Fracassi C, Eusebi F, Rossini PM (2008) White matter vascular lesions are related to parietal-to-frontal coupling of EEG rhythms in mild cognitive impairment. Hum Brain Mapp 29(12):1355–1367

Babiloni C, Lizio R, Marzano N, Capotosto P, Soricelli A, Triggiani AI, Cordone S, Gesualdo L, Del Percio C (2016) Brain neural

synchronization and functional coupling in Alzheimer's disease as revealed by resting state EEG rhythms. Int J Psychophysiol 103:88–102. https://doi.org/10.1016/j.ijpsycho.2015.02.008 (**Epub 2015 Feb 7. PMID: 25660305**)

Barry RJ, De Blasio FM (2017) EEG differences between eyes-closed and eyes-open resting remain in healthy ageing. Biol Psychol 129:293–304. https://doi.org/10.1016/j.biopsycho.2017.09.010

Barttfeld P, Amoruso L, Ais J, Cukier S, Bavassi L, Tomio A, Manes F, Ibañez A, Sigman M (2013) Organization of brain networks governed by long-range connections index autistic traits in the general population. J Neurodegener Disord 5(1):16. https://doi.org/10.1186/1866-1955-5-16 (**PMID:23806204;PMCID: PMC3698083**)

Barttfeld P, Petroni A, Báez S, Urquina H, Sigman M, Cetkovich M, Torralva T, Torrente F, Lischinsky A, Castellanos X, Manes F, Ibañez A (2014) Functional connectivity and temporal variability of brain connections in adults with attention deficit/hyperactivity disorder and bipolar disorder. Neuropsychobiology 69(2):65–75. https://doi.org/10.1159/000356964 (**Epub 2014 Feb 27 PMID: 24576926**)

Bassett DS, Bullmore E (2006) Small-world brain networks. Neuroscientist 12(6):512–523. https://doi.org/10.1177/1073858406293182

Bastos AM, Schoffelen JM (2016) A tutorial review of functional connectivity analysis methods and their interpretational pitfalls. Front Syst Neurosci. https://doi.org/10.3389/fnsys.2015.00175

Berger H (1929) Uber das Elektrenkephalogramm des Menschen. Archiv f Psychiatrie. https://doi.org/10.1007/BF01797193

Bisiach E, Luzzatti C (1978) Unilateral neglect of representational space. Cortex 14(1):129–133

Bola M, Gall C, Moewes C, Fedorov A, Hinrichs H, Sabel BA (2014) Brain functional connectivity network breakdown and restoration in blindness. Neurology 83(6):542–551. https://doi.org/10.1212/WNL.0000000000000672

Bola M, Gall C, Sabel BA (2015) Disturbed temporal dynamics of brain synchronization in vision loss. Cortex 67:134–146. https://doi.org/10.1016/j.cortex.2015.03.020

Bollimunta A, Chen Y, Schroeder CE, Ding M (2008) Neuronal mechanisms of cortical alpha oscillations in awake-behaving macaques. J Neurosci 28(40):9976–9988. https://doi.org/10.1523/JNEUROSCI.2699-08.2008 (**PMID: 18829955; PMCID: PMC2692971**)

Bolognini N, Rasi F, Coccia M, Làdavas E (2005) Visual search improvement in hemianopic patients after audio-visual stimulation. Brain 128(12):2830–2842. https://doi.org/10.1093/brain/awh656

Bueichekú E, Miró-Padilla A, Ávila C (2020) Functional connectivity at rest captures individual differences in visual search. Brain Struct Funct 225:537–549. https://doi.org/10.1007/s00429-019-02008-2

Caliandro P, Vecchio F, Miraglia F, Reale G, Della Marca G, La Torre G, Lacidogna G, Iacovelli C, Padua L, Bramanti P, Rossini PM (2017) Small-world characteristics of cortical connectivity changes in acute stroke. Neurorehabil Neural Repair 31(1):81–94. https://doi.org/10.1177/1545968316662525 (**Epub 2016 Aug 10. PMID: 27511048**)

Cantero JL, Atienza M, Salas RM (2002) Human alpha oscillations in wakefulness, drowsiness period, and REM sleep: different electroencephalographic phenomena within the alpha band. Clin Neurophysiol 32(1):54–71. https://doi.org/10.1016/s0987-7053(01)00289-1 (**PMID: 11915486**)

Capilla A, Schoffelen J-M, Paterson G, Thut G, Gross J (2014) Dissociated α-band modulations in the dorsal and ventral visual pathways in visuospatial attention and perception. Cereb Cortex 24(2):550–561. https://doi.org/10.1093/cercor/bhs343

Castellanos NP, Paúl N, Ordóñez VE, Demuynck O, Bajo R, Campo P, Bilbao A, Ortiz T, del Pozo F, Maestú F (2010) Reorganization of functional connectivity as a correlate of cognitive recovery in acquired brain injury. Brain 133(8):2365–2381. https://doi.org/10.1093/brain/awq174

Cecere R, Rees G, Romei V (2015) Individual differences in alpha frequency drive crossmodal illusory perception. Curr Biol 25(2):231–235. https://doi.org/10.1016/j.cub.2014.11.034

Cohen MX (2014) Analyzing neural time series data: theory and practice. MIT Press, Cambridge

Cooke J, Poch C, Gillmeister H, Costantini M, Romei V (2019) Oscillatory properties of functional connections between sensory areas mediate cross-modal illusory perception. J Neurosci 39(29):5711–5718. https://doi.org/10.1523/JNEUROSCI.3184-18.2019

Corballis PM, Funnell MG, Gazzaniga MS (2002) Hemispheric asymmetries for simple visual judgments in the split brain. Neuropsychologia 40(4):401–410. https://doi.org/10.1016/s0028-3932(01)00100-2

Dawson KA (2004) Temporal organization of the brain: neurocognitive mechanisms and clinical implications. Brain Cogn 54(1):75–94. https://doi.org/10.1016/S0278-2626(03)00262-8

Delorme A, Makeig S (2004) EEGLAB: an open source toolbox for analysis of single-trial EEG dynamics including independent component analysis. J Neurosci Methods 134(1):9–21. https://doi.org/10.1016/J.JNEUMETH.2003.10.009

Doesburg SM, Green JJ, McDonald JJ, Ward LM (2009) From local inhibition to long-range integration: a functional dissociation of alpha-band synchronization across cortical scales in visuospatial attention. Brain Res 1303:97–110. https://doi.org/10.1016/j.brainres.2009.09.069

Dottori M, Sedeño L, Martorell Caro M, Alifano F, Hesse E, Mikulan E, García AM, Ruiz-Tagle A, Lillo P, Slachevsky A, Serrano C, Fraiman D, Ibañez A (2017) Towards affordable biomarkers of frontotemporal dementia: a classification study via network's information sharing. Sci Rep. https://doi.org/10.1038/s41598-017-04204-8

Dubovik S, Pignat J-M, Ptak R, Aboulafia T, Allet L, Gillabert N, Magnin C et al (2012) The behavioral significance of coherent resting-state oscillations after stroke. Neuroimage 61(1):249–257. https://doi.org/10.1016/j.neuroimage.2012.03.024

Dundon NM, Bertini C, Làdavas E, Sabel BA, Gall C (2015b) Visual rehabilitation: visual scanning, multisensory stimulation and vision restoration trainings. Front Behav Neurosci 9:192

Dundon NM, Làdavas E, Maier ME, Bertini C (2015a) Multisensory stimulation in hemianopic patients boosts orienting responses to the hemianopic field and reduces attentional resources to the intact field. Restor Neurol Neurosci 33(4):405–419

Fingelkurts AA, Fingelkurts AA, Rytsälä H, Suominen K, Isometsä E, Kähkönen S (2007) Impaired functional connectivity at EEG alpha and theta frequency bands in major depression. Hum Brain Mapp 28:247–261. https://doi.org/10.1002/hbm.20275

Friston KJ (2011) Functional and effective connectivity: a review. Brain Connect 1(1):13–36. https://doi.org/10.1089/brain.2011.0008 (**PMID: 22432952**)

Gallina J, Pietrelli M, Zanon M, Bertini C (2021) Hemispheric differences in altered reactivity of brain oscillations at rest after posterior lesions. Brain Struct Funct. https://doi.org/10.1007/s00429-021-02279-8

Gallotto S, Duecker F, Oever ST, Schuhmann T, de Graaf TA, Sack AT (2020) Relating alpha power modulations to competing visuospatial attention theories. Neuroimage 207:116429. https://doi.org/10.1016/j.neuroimage.2019.116429

Gitelman DR, Nobre AC, Parrish TB, LaBar KS, Kim YH, Meyer JR, Mesulam M (1999) A large-scale distributed network for covert spatial attention: further anatomical delineation based on

stringent behavioural and cognitive controls. Brain 122(6):1093–1106. https://doi.org/10.1093/brain/122.6.1093

Grasso PA, Làdavas E, Bertini C (2016) Compensatory recovery after multisensory stimulation in hemianopic patients: behavioral and neurophysiological components. Front Syst Neurosci. https://doi.org/10.3389/fnsys.2016.00045

Grasso PA, Pietrelli M, Zanon M, Làdavas E, Bertini C (2020a) Alpha oscillations reveal implicit visual processing of motion in hemianopia. Cortex 122:81–96. https://doi.org/10.1016/j.cortex.2018.08.009

Grasso PA, Gallina J, Bertini C (2020b) Shaping the visual system: Cortical and subcortical plasticity in the intact and the lesioned brain. Neuropsychologia. https://doi.org/10.1016/j.neuropsychologia.2020.107464

Greicius MD, Krasnow B, Reiss AL, Menon V (2003) Functional connectivity in the resting brain: a network analysis of the default mode hypothesis. PNAS 100(1):253–258. https://doi.org/10.1073/pnas.0135058100

Guggisberg AG, Honma SM, Findlay AM, Dalal SS, Kirsch HE, Berger MS, Nagarajan SS (2008) Mapping functional connectivity in patients with brain lesions. Ann Neurol 63:193–203. https://doi.org/10.1002/ana.21224

Guggisberg AG, Rizk S, Ptak R (2015) Two intrinsic coupling types for resting-state integration in the human brain. Brain Topogr 28:318–329

Guo X, Jin Z, Feng X, Tong S (2014) Enhanced effective connectivity in mild occipital stroke patients with hemianopia. IEEE Trans Neural Syst Rehabil Eng 22(6):1210–1217. https://doi.org/10.1109/TNSRE.2014.2325601

Haig AR, Gordon E, De Pascalis V, Meares RA, Bahramali H, Harris H (2000) Gamma activity in schizophrenia: evidence of impaired network binding? Clin Neurophysiol 111(8):1461–1468. https://doi.org/10.1016/S1388-2457(00)00347-3

Hardmeier M, Hatz F, Bousleiman H, Schindler C, Stam CJ, Fuhr P (2014) Reproducibility of functional connectivity and graph measures based on the phase lag index (PLI) and weighted phase lag index (WPLI) derived from high resolution EEG. PLoS ONE 9(10):e108648. https://doi.org/10.1371/journal.pone.0108648

Heilman KM, Valenstein E (1979) Mechanisms underlying hemispatial neglect. Ann Neurol 5(2):166–170

Heilman KM, Valenstein E, Watson RT (1984) Neglect and related disorders. Semina Neurol 4(2):209–219

Hindriks R, Woolrich M, Luckhoo H, Joensson M, Mohseni H, Kringelbach ML, Deco G (2015) Role of white-matter pathways in coordinating alpha oscillations in resting visual cortex. Neuroimage 106:328–339. https://doi.org/10.1016/j.neuroimage.2014.10.057

Jewell G, McCourt ME (2000) Pseudoneglect: a review and meta-analysis of performance factors in line bisection tasks. Neuropsychologia 38(1):93–110. https://doi.org/10.1016/s0028-3932(99)00045-7

Kayser J, Tenke CE (2015) On the benefits of using surface laplacian (current source density) methodology in electrophysiology. Int J Psychophysiol 97(3):171–173. https://doi.org/10.1016/j.ijpsycho.2015.06.001

Klimesch W, Sauseng P, Hanslmayr S (2007) EEG alpha oscillations: the inhibition–timing hypothesis. Brain Res Rev 53(1):63–88. https://doi.org/10.1016/J.BRAINRESREV.2006.06.003

Làdavas E, Tosatto L, Bertini C (2020) Behavioural and functional changes in neglect after multisensory stimulation. Neuropsychol Rehabil. https://doi.org/10.1080/09602011.2020.1786411

Ma J, Lin Y, Hu C et al (2021) Integrated and segregated frequency architecture of the human brain network. Brain Struct Funct 226:335–350. https://doi.org/10.1007/s00429-020-02174-8

Mattingley JB, Bradshaw JL, Nettleton NC, Bradshaw JA (1994) Can task specific perceptual bias be distinguished from unilateral neglect? Neuropsychologia 32(7):805–817

McCourt ME, Jewell G (1999) Visuospatial attention in line bisection: stimulus modulation of pseudoneglect. Neuropsychologia 37(7):843–855. https://doi.org/10.1016/s0028-3932(98)00140-7

McCourt ME, Olafson C (1997) Cognitive and perceptual influences on visual line bisection: psychophysical and chronometric analyses of pseudoneglect. Neuropsychologia 35(3):369–380. https://doi.org/10.1016/S0028-3932(96)00143

Melloni M, Sedeño L, Hesse E et al (2015) Cortical dynamics and subcortical signatures of motor-language coupling in Parkinson's disease. Sci Rep 5:11899. https://doi.org/10.1038/srep11899

Metzen D, Genç E, Getzmann S et al (2022) Frontal and parietal EEG alpha asymmetry: a large-scale investigation of short-term reliability on distinct EEG systems. Brain Struct Funct 227:725–740. https://doi.org/10.1007/s00429-021-02399-1

Minami S, Amano K (2017) Illusory jitter perceived at the frequency of alpha oscillations. Curr Biol 27(15):2344-2351.e4. https://doi.org/10.1016/j.cub.2017.06.033

Nicholls ME, Roberts GR (2002) Can free-viewing perceptual asymmetries be explained by scanning, pre-motor or attentional biases? Cortex 38(2):113–136. https://doi.org/10.1016/s0010-9452(08)70645-2

Nobre AC, Sebestyen GN, Gitelman DR, Mesulam MM, Frackowia RS, Frith CD (1997) Functional localization of the system for visuospatial attention using positron emission tomography. Brain 120(3):515–533. https://doi.org/10.1093/brain/120.3.515

Onnela JP, Saramäki J, Kertész J, Kaski K (2005) Intensity and coherence of motifs in weighted complex networks. Phys Rev E 71:065103(R)

Palva S, Palva JM (2007) New vistas for α-frequency band oscillations. Trends Neurosci 30(4):150–158. https://doi.org/10.1016/j.tins.2007.02.001

Parra MA, Mikulan E, Trujillo N, Sala SD, Lopera F, Manes F, Starr J, Ibanez A (2017) Brain information sharing during visual short-term memory binding yields a memory biomarker for familial Alzheimer's disease. Curr Alzheimer Res 14(12):1335–1347. https://doi.org/10.2174/1567205014666617 0614163316 (**PMID: 28641509**)

Passamonti C, Bertini C, Làdavas E (2009) Audio-visual stimulation improves oculomotor patterns in patients with hemianopia. Neuropsychologia 47(2):546–555

Pedersini CA, Guàrdia-Olmos NJ, Montalà-Flaquer M, Cardobi N, Sanchez-Lopez J, Parisi G, Savazzi S, Marzi CA (2020) Functional interactions in patients with hemianopia: a graph theory-based connectivity study of resting fMRI signal. PLoS ONE. https://doi.org/10.1371/journal.pone.0226816

Pfurtscheller G, Neuper C, Mohl W (1994) Event-related desynchronization (ERD) during visual processing. Int J Psychophysiol 16(2):147–153. https://doi.org/10.1016/0167-8760(89)90041-X

Pietrelli M, Zanon M, Làdavas E, Grasso PA, Romei V, Bertini C (2019) Posterior brain lesions selectively alter alpha oscillatory activity and predict visual performance in hemianopic patients. Cortex 121:347–361. https://doi.org/10.1016/j.cortex.2019.09.008

Romei V, Brodbeck V, Michel C, Amedi A, Pascual-Leone A, Thut G (2008a) Spontaneous fluctuations in posterior α-band EEG activity reflect variability in excitability of human visual areas. Cereb Cortex 18(9):2010–2018. https://doi.org/10.1093/cercor/bhm229

Romei V, Rihs T, Brodbeck V, Thut G (2008b) Resting electroencephalogram alpha-power over posterior sites indexes baseline visual cortex excitability. Neuro Rep 19(2):203. https://doi.org/10.1097/WNR.0b013e3282f454c4

Rorden C, Brett M (2000) Stereotaxic display of brain lesions. Behav Neurol 12(4):191–200. https://doi.org/10.1155/2000/421719

Rorden C, Karnath HO, Bonilha L (2007) Improving lesion-symptom mapping. J Cogn Neurosci 19(7):1081–1088. https://doi.org/10.1162/jocn.2007.19.7.1081

Rosanova M, Casali A, Bellina V, Resta F, Mariotti M, Massimini M (2009) Natural frequencies of human corticothalamic circuits. J Neurosci 29(24):7679–7685. https://doi.org/10.1523/JNEUROSCI.0445-09.2009

Rossini PM, Rossi S, Babiloni C, Polich J (2007) Clinical neurophysiology of aging brain: from normal aging to neurodegeneration. Prog Neurobiol 83(6):375–400. https://doi.org/10.1016/j.pneurobio.2007.07.010

Rubinov M, Sporn O (2010) Complex network measures of brain connectivity: uses and interpretations. Neuroimage 52:1059–1069

Sadaghiani S, Kleinschmidt A (2016) Brain networks and α-oscillations: structural and functional foundations of cognitive control. Trends Cogn Sci 20(11):805–817. https://doi.org/10.1016/j.tics.2016.09.004

Samaha J, Postle BR (2015) The speed of alpha-band oscillations predicts the temporal resolution of visual perception. Curr Biol 25(22):2985–2990. https://doi.org/10.1016/j.cub.2015.10.007

SanchezLopez J, Savazzi S, Pedersini CA, Cardobi N, Marzi CA (2020) Neural bases of unconscious orienting of attention in hemianopic patients: hemispheric differences. Cortex 127:269–289. https://doi.org/10.1016/j.cortex.2020.02.015

Sporns O (2011) The human connectome: a complex network. Ann N Y Acad Sci 1224:109–125. https://doi.org/10.1111/j.1749-6632.2010.05888.x

Stam CJ (2010) Characterization of anatomical and functional connectivity in the brain: a complex networks perspective. Int J Psychophysiol 77(3):186–194. https://doi.org/10.1016/j.ijpsycho.2010.06.024

Stam CJ, Nolte G, Daffertshofer A (2007) Phase lag index: assessment of functional connectivity from multi channel EEG and MEG with diminished bias from common sources. Hum Brain Mapp 11:1178–1193. https://doi.org/10.1002/hbm.20346

Strogatz FH (2001) Exploring complex networks. Nature 410:268–276. https://doi.org/10.1038/35065725

Thut G, Veniero D, Romei V, Miniussi C, Schyns P, Gross J (2011) Rhythmic TMS causes local entrainment of natural oscillatory signatures. Curr Biol 21(14):1176–1185. https://doi.org/10.1016/j.cub.2011.05.049

Tononi G, Edelman GM (1998) Consciousness and complexity. Science 282(5395):1846–1851. https://doi.org/10.1126/science.282.5395.1846

Tononi G, Sporns O, Edelman GM (1994) A measure for brain complexity: relating functional segregation and integration in the nervous system. PNAS 91(11):5033–5037. https://doi.org/10.1073/pnas.91.11.5033

van Diessen E, Numan T, van Dellen E, van der Kooi A, Boersma M, Hofman D et al (2015) Opportunities and methodological challenges in EEG and MEG resting state functional brain network research. Clin Neurophysiol 126:1468–1481. https://doi.org/10.1016/j.clinph.2014.11.018

Varela F, Lachaux JP, Rodriguez E, Martinerie J (2001) The brainweb: phase synchronization and large-scale integration. Nat Rev Neurosci 2:229–239

Vecchio F, Caliandro P, Reale G, Miraglia F, Piludu F, Masi G, Iacovelli C, Simbolotti C, Padua L, Leone E, Alù F, Colosimo C, Rossini PM (2019a) Acute cerebellar stroke and middle cerebral artery stroke exert distinctive modifications on functional cortical connectivity: a comparative study via EEG graph theory. Clin Neurophysiol 130(6):997–1007. https://doi.org/10.1016/j.clinph.2019a.03.017 (**Epub 2019 Apr 6. PMID: 31005052**)

Vecchio F, Tomino C, Miraglia F, Iodice F, Erra C, Di Iorio R, Judica E, Alù F, Fini M, Rossini PM (2019b) Cortical connectivity from EEG data in acute stroke: a study via graph theory as a potential biomarker for functional recovery. Int J Psychophysiol 146:133–138. https://doi.org/10.1016/j.ijpsycho.2019b.09.012 (**Epub 2019 Oct 21. PMID: 31648028**)

Venskus A, Ferri F, Migliorati D, Spadone S, Costantini M, Hughes G (2021) Temporal binding window and sense of agency are related processes modifiable via occipital tACS. PLoS ONE 16(9):e0256987. https://doi.org/10.1371/journal.pone.0256987

Vinck M, Oostenveld R, van Wingerden M, Battaglia F, Pennartz CMA (2011) An improved index of phase-synchronization for electrophysiological data in the presence of volume-conduction. Noise and sample-size bias. Neuroimage 55(4):1548–1565. https://doi.org/10.1016/j.neuroimage.2011.01.055

von Stein A, Sarnthein J (2000) Different frequencies for different scales of cortical integration: from local gamma to long range alpha/theta synchronization. Int J Psychophysiol 38(3):301–313. https://doi.org/10.1016/s0167-8760(00)00172-0 (**PMID: 11102669**)

Wang L, Xiaoli G, Sun J, Jin Z, Tong S (2012) Cortical networks of hemianopia stroke patients: a graph theoretical analysis of EEG signals at resting state. Conference proceedings: annual international conference of the IEEE engineering in medicine and biology society. Ann Conf IEEE Eng Med Biol Soc 2012:49–52. https://doi.org/10.1109/EMBC.2012.6345868

Watts DJ, Strogatz SH (1998) Collective dynamics of 'small-world' networks. Nature 393:440–442

Westlake KP, Hinkley LB, Bucci M, Guggisberg AG, Byl N, Findlay AM, Henry RG, Nagarajan SS (2012) Resting state α-band functional connectivity and recovery after stroke. Exp Neurol 237(1):160–169. https://doi.org/10.1016/j.expneurol.2012.06.020 (**Epub 2012 Jun 27. Erratum in: Experimental Neurology, 238(2):100. PMID: 22750324; PMCID: PMC3646713**)

Wilson B, Cockburn J, Halligan P (1987) Development of a behavioral test of visuospatial neglect. Arch Phys Med Rehabil 68(2):98–102

Wu W, Sun J, Jin Z, Guo X, Qiu Y, Zhu Y, Tong S (2011) Impaired neuronal synchrony after focal ischemic stroke in elderly patients. Clin Neurophysiol 122(1):21–26. https://doi.org/10.1016/j.clinph.2010.06.003

Wutz A, Samaha J, Melcher D (2018) Frequency modulation of neural oscillations according to visual task demands. PNAS. 115(6):1346–1351. https://doi.org/10.1073/pnas.1713318115

Zhang Y, Zhang Y, Cai P, Luo H, Fang F (2019) The causal role of α-oscillations in feature binding. PNAS 116:17023–17028. https://doi.org/10.1073/pnas.1904160116

Publisher's Note Springer Nature remains neutral with regard to jurisdictional claims in published maps and institutional affiliations.